duration. Energy conversion efficiency from the incident UV beam is about 30 percent. Full width of crystal angle at half maximum output power for fixed incident wavelengths was approximately 3 mrad, which roughly coincides with angle divergence of the incident IR Raman beam. This means that the conversion efficiency is not strictly limited by the acceptance angle of the KDP crystal. Transmission of the KDP crystal measured with a Varian Cary 2300 spectrophotometer is 60-50 percent between 200 and 190 nm. Taking the energy loss due to absorption into account, conversion efficiency in the three-wave interaction will reach 50 percent.

An alternative configuration in sum-frequency generation was investigated, which provided even higher output energy compared to the above configuration in the tuning ranges of 192-195 and 198-202 nm. The nitrogen Raman cell and related optical components were removed from the middle line in Fig. 2 and the fundamental and the nitrogen or hydrogen Raman radiation of the top line were frequency-mixed in a type-1 KDP crystal of 1.5 cm length with a 77° cut. A sum-frequency beam at 223.9 or 233.4 nm gave an energy of 0.5 mJ in both cases and was mixed further with the optical parametric radiation by using a type-1 KDP crystal of 1.5 cm length with a 77° cut. The output energy was approximately 40 μJ. The high-frequency sides of the two tuning ranges were limited by phase-matching and the low-frequency sides by the tuning range of the OPG. The difference in the output energies of the two different configurations is probably due to a difference in the incident energies of the tunable UV beam (0.1 mJ) and the optical parametric beam (0.5 mJ).

In summary, we have obtained, by picosecond sum-frequency mixing, short wavelength tunable UV radiation. The results show that KDP is suitably used in sum-frequency mixing to generate radiation with wavelength close to the UV absorption edge instead of using expensive crystals which can be phase-matched in this spectral region such as potassium pentaborate, urea, and beryllium sulphate.

References

[1] G. A. Massey and J. C. Johnson, "Wavelength-tunable optical mixing experiments between 208 and 259 nm," *IEEE J. Quantum Electron.*, vol. QE-12, pp. 721-727, 1976.

[2] F. B. Dunning and R. E. Stickel, Jr., "Sum frequency mixing in potassium pentaborate as a source of tunable coherent radiation at wavelengths below 217 nm," *Appl. Opt.*, vol. 15, pp. 3131-3134, 1976.

[3] H. J. Dewey, "Second harmonic generation in $KB_5O_8 \cdot 4H_2O$ from 217.1 to 315.0 nm," *IEEE J. Quantum Electron.*, vol. QE-12, pp. 303-306, 1976.

[4] K. Kato, "Tunable uv generation in $KB_5O_8 \cdot 4H_2O$ to 1966 Å," *Appl. Phys. Lett.*, vol. 30, p. 583, 1977.

[5] F. B. Dunning, "Ultraviolet generation by sum frequency mixing," *Laser Focus*, vol. 14, pp. 72-76, 1978.

[6] R. E. Stickel, Jr., and F. B. Dunning, "Generation of tunable coherent vacuum uv radiation in KB5," *Appl. Opt.*, vol. 17, pp. 981-982, 1978.

[7] J. M. Halbout, S. Blit, W. Donaldson, and C. L. Tang, "Efficient phase-matched second harmonic generation and sum-frequency mixing in urea," *IEEE J. Quantum Electron.*, vol. QE-15, pp. 1176-1180, 1979.

[8] Y. Takagi, M. Sumitani, N. Nakashima, D. V. O'Connor, and K. Yoshihara, "Generation of high-power picosecond continuously tunable radiation between 215 and 245 nm by mixing of Raman and optical parametric light," *Appl. Phys. Lett.*, vol. 42, pp. 489-491, 1983.

[9] G. C. Ghosh and G. C. Bhar, "Temperature dispersion in ADP, KDP, and KD*P for nonlinear devices," *IEEE J. Quantum Electron.*, vol. QE-18, pp. 143-145, Feb. 1982.

[10] F. Zernike, Jr., "Refractive indices of ammonium dihydrogen phosphate and potassium dihydrogen phosphate between 2000 Å and 1.5 μ," *J. Opt. Soc. Amer.*, vol. 54, pp. 1215-1220, 1964.

Papers

Single-Frequency, Single-Knob Tuning of a CW Color Center Laser

NILSON DIAS VIEIRA, JR. AND LINN F. MOLLENAUER, MEMBER, IEEE

Abstract—**We describe a simple way to achieve CW single-frequency laser operation with a grating as the sole tuning element. It is shown, both experimentally and theoretically, that by proper choice of cavity parameters, the competing hole burning modes can be completely suppressed. Experiments to demonstrate the theoretical calculations were carried out in a CW color center laser using $Tl^0(1)$ centers. Linewidths of 0.01 cm^{-1} were obtained and this figure can probably be much improved by proper cavity stabilization. The method can be readily extended to any compact gain medium.**

Manuscript received April 9, 1984; revised November 13, 1984. This work was supported in part by the Brazilian Nuclear Energy Commission.

N. D. Vieira, Jr. was with AT&T Bell Laboratories, Holmdel, NJ 07733, on leave from the Instituto de Pesquisa Energeticas e Nucleares, Sao Paulo, Brazil.

L. F. Mollenauer is with AT&T Bell Laboratories, Holmdel, NJ 07733,

I. Introduction

We describe here a simple way to combine one knob tuning with true single-frequency operation of broadly

0018-9197/85/0300-0195$01.00

tunable lasers. (By "single-frequency" operation we mean, of course, not the impossible goal of infinitesimal linewidth, but rather the achievement of lasing on just one longitudinal mode at a time.) In our scheme, tuning is accomplished through rotation of the sole tuning element, a grating used in the Littrow configuration. With its ability to tune continuously over large frequency spans, a laser operated according to this scheme is suited for many applications, such as the survey of complex spectra, or the characterization of integrated optic devices [1]. We have been able to demonstrate successful application of the scheme in experiments carried out with a CW color center laser; however, the scheme should work equally well in any laser using a compact, homogeneously broadened gain medium.

As is well known, to obtain single-frequency operation in a standing wave cavity, one must overcome the effects of *spatial hole burning* [2]-[6]. That is, intensity nodes of the desired mode produce build-up of inverted population in the gain medium, such that other longitudinal modes have the potential to compete successfully. To suppress these unwanted modes, it is usual to employ one or more internal etalons in addition to the prism, grating, or other element used for wide band tuning [7]. However, the small free spectral range of the etalon, and the need for combined tuning of several elements, lead to complex and cumbersome operation.

Of course, the problem of spatial hole burning can be circumvented through use of a ring laser [2]. There, unidirectional traveling waves homogeneously depopulate the gain medium along the direction of propagation. Although single-frequency operation is easily attained [8], [9] in such ring lasers, the Faraday rotator and other elements required to guarantee unidirectional operation are often expensive, cumbersome and lossy. (This is especially true in the infrared.)

In our scheme, single-frequency operation is obtained in a simple standing wave cavity by virtue of the following.

1) The cavity end mirror is placed as close as possible (~3.7 mm in our color center laser) to the gain medium, in order to obtain maximum possible frequency separation between the desired modes and the modes offering the most serious potential for competition.

2) The depth of illuminated grating, and hence its selectivity, are sufficiently great to completely suppress operation on all possible competing modes. The proper grating illumination is obtained through use of a two-mirror internal telescope to expand the beam (to ~3-5 mm in our experiments), and through choice of grating groove spacing such that the grating angle will be large enough (see Fig. 1).

Zeroth order reflection from the grating is used for output, where a second plane mirror, rotated with the grating, provides a steady beam direction and location [10], [11]. Thus, the output beam has the same expanded size as that impinging on the grating. Still small enough to be readily compatible with most laboratory optics, the expanded output beam has a larger than usual confocal parameter. Hence it has a less rapidly changing size, and is more readily focused into a tight diffraction limited spot; both properties are often desirable. The major disadvantage of our scheme lies in the fact that the output frequency fluctuates more severely with vibration and other cavity disturbances than in the cavity using etalons. In our experiments, for example, the attained time-average line width was ~0.01 cm^{-1}, a figure much in excess of that attained in the best single-frequency lasers. However, this figure could be greatly improved with better mechanical and thermal design. (Short term frequency definition was much better than the above mentioned figure.) On the other hand, frequency definition to 0.01 cm^{-1} is already more than good enough for many purposes.

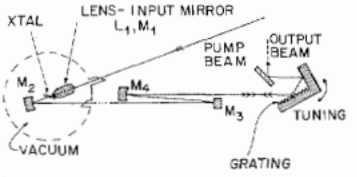

Fig. 1. Diagram of the coaxially pumped cavity with the internal magnifying telescope (consisting of convex mirror M_3 and concave mirror M_4). Vacuum is provided in order to isolate the crystal liquid nitrogen temperature. (Although it may not be evident from the drawing, the lens-input mirror element is separated from the crystal by a small gap.)

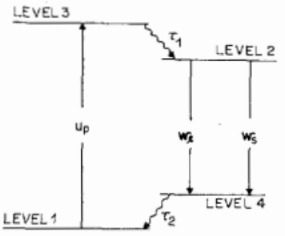

Fig. 2. Simplified diagram of the pumping optical cycle. Centers are excited in the normal configuration (levels 1-3) with a pumping rate u_p, and decay from level 2 by spontaneous emission (decay rate w_l) and stimulated emission (decay rate w_s).

II. Theoretical

In this section we treat the problem of spatial hole burning and its consequences, under the assumption that only one mode is lasing, i.e., that we have already achieved true single-frequency operation. The treatment proceeds as follows. First, we calculate the spatial population modulation due to the standing wave, then the relative gain for other frequencies resulting from the population modulation. Finally, we multiply that gain by the frequency response of the grating to obtain the net gain. The criterion for single-frequency operation is, of course, that the curve of the net gain versus frequency have just one maximum, located at the lasing frequency. On the other hand, where the maxima lie elsewhere, there will then be simultaneous lasing on several frequencies. We show that the spacing of these frequencies is equal to the quantity $c/4d$ (where d is the distance between the gain medium and the closest mirror) only when the grating band pass is much wider than that quantity.

A. Spatial Population Distribution

The gain medium is assumed to be a nearly perfect four level system. As shown in Fig. 2, the nonradiative decay times τ_1 and τ_2 are very short, such that $1/\tau_{1,2} \gg w_l + w_s$ where w_l is the luminescent decay rate and w_s is the stimulated decay rate

in the presence of the laser field. Thus, we have

$$N_1 + N_2 = N_0 \tag{1}$$

where N_1 and N_2 are the densities of centers in the 1 and 2 levels, respectively, and N_0 is the total concentration of laser active centers.

The rate equation describing the optical cycle is

$$\dot{N}_1 = -u_p N_1 + (w_l + w_s) N_2 \tag{2}$$

where u_p is the optical pumping rate, and where we neglect the radial dependence of the pump and laser mode by supposing an impinging plane wave. It can be shown that this approximation leads to an upper limit in the calculated gain and it becomes more valid when the laser is operating well above the threshold, i.e., when $w_s, u_p \gg w_l$.

Let the wavevector of the single lasing mode be k_o. Then the intracavity standing wave intensity in the gain medium is given by

$$I = I_{\max} \sin^2 (k_o nz) \tag{3}$$

where z is the distance along the propagation direction, n is the refractive index, and $I_{\max}$ is a slowly varying z-dependent function. Therefore, the stimulated decay rate is given by

$$w_s = \sigma I = \sigma I_{\max} \sin^2 (k_0 nz) \tag{4}$$

where σ is the luminescence cross section. Taking $w_{\max} = \sigma I_{\max}$, substituting (4) into (2), and imposing the steady-state condition ($\dot{N}_1 = 0$), we obtain the inverted population along the gain medium

$$N_2(z) = \frac{u_p N_0}{u_p + w_l + w_{\max} \sin^2 (k_0 nz)}. \tag{5}$$

From (5) we can immediately see that the population N_2 varies with half the spatial period of the field, between the values $N_{\min}$ and $N_{\max}$ given by

$$N_{\max} = \frac{u_p N_0}{u_p + w_l} \tag{6}$$

in the nulls of the laser field and

$$N_{\min} = \frac{u_p N_0}{u_p + w_l + w_{\max}} \tag{7}$$

where the stimulated emission is at its greatest.

B. Gain Analysis

To determine if a potentially competing mode is capable of lasing, we must first calculate the gain available to it in the presence of the population distribution just calculated [see (5)]. In the gain region, the two modes differ by a phase shift ϕ accumulated over the distance d between the closest mirror and the gain medium itself. (The phases must be the same at the mirror, where there is a null in the electrical fields.) For simplicity, we make the assumption that the gain medium is so thin, and the two frequencies in question are so close, that ϕ is essentially a constant within the gain region. Although the assumption is not truly correct, it overestimates the gain available to the competing mode, and hence is a conservative assumption for our purposes. In any event, as ϕ increases with increasing separation between the two modes, the sinusoidal intensity profile scans across the fixed population distribution profile. The maximum gain of the competing mode is attained when its intensity peaks coincide with the peaks of the population distribution.

The phase shift ϕ is given by

$$\phi = \Delta k\, d = \frac{\pi}{2} \frac{\Delta \nu}{\Delta \nu_{hb}} \tag{8}$$

where $\Delta \nu_{hb} = (c/4d)$ is the well-known "hole burning frequency spacing" and $\Delta \nu$ is the frequency difference between the main and competing modes.

The stimulated decay rate for the competing mode (intensity I' in photons centimeters^{-2} · seconds^{-1}) is given by

$$w(z) = \sigma I'_{\max} \sin^2 (k_o nz + \phi). \tag{9}$$

The small signal gain coefficient is computed by taking an average over one half optical period

$$g(\phi, z) = \frac{4}{\lambda} \int_z^{z+\lambda/2} \frac{w(z')}{I'_{\max}} N_2(z')\, dz' \tag{10}$$

or, substituting for $N_2(z)$ from (5), we write

$$g(\phi) = \frac{2\sigma N_0 u_p}{\pi} \int_o^{\pi} \frac{\sin^2 (\theta + \phi)\, d\theta}{u_p + w_l + w_{\max} \sin^2 \theta}. \tag{11}$$

Note that g is now independent of z due to the assumed uniform behavior of $N_2(z)$. Thus, the overall gain is given by

$$\frac{I'_{\max}(L)}{I'_{\max}(O)} = \exp \{g(\phi) L\} \tag{12}$$

where L is the length of the gain path.

After further simplification and integration, from (11) we obtain

$$g(\phi) = \sigma N_{\min} G \left[1 - \left(\frac{G-1}{G+1}\right) \cos (2\phi)\right] \tag{13}$$

where

$$G = \sqrt{\frac{N_{\max}}{N_{min}}}. \tag{14}$$

For $\phi = 0$, g is the gain coefficient of the fundamental mode, and hence is the gain at threshold

$$g_t = 2\sigma N_{\min} \left(\frac{G}{G+1}\right). \tag{15}$$

Substituting (15) into (13), the gain at any given frequency $\nu = \nu_o + \Delta \nu$ can be written as

$$g(\nu) = g_t \left[1 + (G-1) \sin^2 \left(\frac{\pi}{2} \frac{\Delta \nu}{\Delta \nu_{hb}}\right)\right]. \tag{16}$$

Note that the maximum gain ($g_t G$) is limited by the required gain at threshold and by the maximum available center density, i.e., G is always less than $\sqrt{N_o/N_{\min}}$, a quantity *independent of the pump power.*

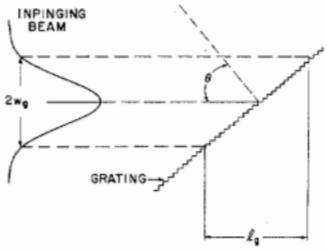

Fig. 3. Gaussian beam with radius w_g impinging on a grating at an angle of incidence θ. The illuminated depth of the grating is l_g.

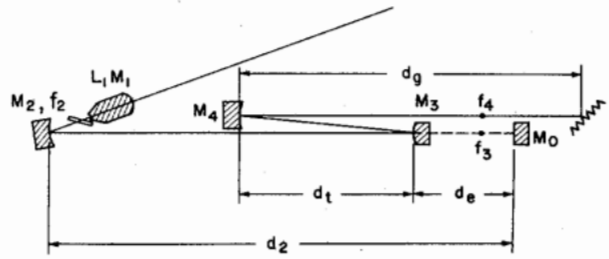

Fig. 4. The cavity of Fig. 1, showing distances relevant to cavity analysis. Mirror M_0 is an equivalent of M_3, M_4 and the grating (see text).

C. Responsivity of the Grating

In order to calculate the grating response, we assume a Gaussian beam profile with a waist radius, w_g, at the grating, and that the first order reflection must lie exactly along the incident beam. For w_g much greater than the groove spacing a, it is easily shown that the response of the grating is

$$R(\nu) = R(\nu_0) \exp\left\{-2\left(\frac{\Delta\nu}{\delta\nu}\right)^2\right\} \tag{17}$$

where ν_0 is the tuned frequency, $\Delta\nu$ as before is the frequency detuning, and $\delta\nu$ is the half width at e^{-2} points of $R(\nu)$, and is given by

$$\delta\nu = \frac{c}{\pi l_g} \tag{18}$$

where l_g is the illuminated depth of grating as shown in Fig. 3. Formally, l_g is given by

$$l_g = 2w_g \tan\theta. \tag{19}$$

Also see Fig. 3 for the definition of θ. A grating operating in the first order of the Littrow configuration is governed by the master equation

$$\lambda = 2a \sin\theta. \tag{20}$$

It is interesting to note that the selectivity of the grating does not depend on the groove spacing but only on the illuminated depth.

D. Condition for Single-Frequency Operation in the Presence of Spatial Hole Burning

By the net gain γ, we mean the product of the gain with all loss factors. Thus, we may write

$$\gamma(\nu) = R(\nu) \exp(2g(\nu) L - \alpha) \tag{21}$$

where α represents the net loss save that associated with the grating. The well-known threshold gain condition is obtained by setting $\gamma(\nu_o)$ equal to unity

$$R(\nu_o) \exp(2g_t L - \alpha) = 1. \tag{22}$$

It is convenient to normalize (21) by (22) and defining $x = \Delta\nu/\Delta\nu_{hb}$; we can write

$$\gamma(x) = \exp\left\{2g_t L(G-1)\sin^2\left(\frac{\pi}{2}x\right) - 2\left(\frac{x}{\beta}\right)^2\right\} \tag{23}$$

where $\beta = \delta\nu/\Delta\nu_{hb}$.

The condition for single-frequency operation is that $\gamma(x)$ have a single maximum occurring at $x = 0$. If this condition is not satisfied, that is, if there are maxima elsewhere, then lasing will also begin to occur at those frequencies as well. (Of course, once such lasing has begun, the population distribution given by (5) will be altered and our analysis no longer applies.) By setting the derivative of (23) equal to zero, we obtain the equation of the maxima

$$\frac{\sin(\pi x)}{x} = \frac{4}{\pi\beta^2} \frac{1}{g_t L(G-1)}. \tag{24}$$

From (24), the *condition for single-frequency operation* can be written as

$$g_t L(G-1) \leqslant \left(\frac{2\Delta\nu_{hb}}{\pi\delta\nu}\right)^2 \tag{25}$$

or

$$g_t L(G-1) \leqslant \left(\frac{l_g}{2d}\right)^2. \tag{26}$$

As noted earlier, the maximum gain G is limited by the total concentration of laser-active centers. Thus, the condition stated in (25) and (26) can always be satisfied by proper choice of cavity parameters.

E. Analysis of the Cavity

In this section we analyze effects of the two-mirror telescope (M_3, M_4) on the three-mirror cavity [12] described in Section I and in Fig. 1. In particular, we calculate the condition for obtaining a stable mode, and its sensitivity to misadjustment of the telescope. We also calculate the telescope magnification, m, and its dependence on cavity parameters.

The first step is to replace the combination of telescope and grating by a single equivalent mirror, M_0. As shown in Fig. 4, let d_g be the spacing between the grating and M_4 (focal length f_4), d_t be the telescope mirror spacing, and (d_e) be the spacing between M_0 and M_3. For convenience, we define a telescope misadjustment parameter

$$\Delta = d_t - f_3 - f_4. \tag{27}$$

(Note that in accordance with the usual sign convention, as the focal length of convex mirror M_3, $f_3 < 0$.) Through a straightforward use of the imaging of optical modes [13] we calculate to first order in Δ

$$d_e = f_3\left[1 + \frac{1}{m_0}\left(\frac{d_g}{f_4} - 1\right)\right] + \frac{1}{m_0^2}\left(\frac{d_g}{f_4} - 1\right)\frac{\Delta}{f_2} \tag{28}$$

where $m_0 = |f_4/f_3|$ is the nominal telescope magnification factor. Note that unless the telescope misadjustment Δ is very large, the last term in (28) is negligible. We also note that d_g is usually comparable in size to f_4; hence the location M_0 is almost always found in the near neighborhood of the focal point of M_3 (see Fig. 4).

The equivalent radius of curvature, R_e, of M_0 is given by

$$R_e = f_3 + d_e + \frac{f_3^2}{\Delta}. \tag{29}$$

Note that, as expected, in the limit of perfect telescope adjustment ($\Delta = 0$), M_0 is a flat mirror.

Using the stability criteria given in [9] for the equivalent resonator, we calculate the stability range $2S$ as

$$2S = \frac{f_2^2}{d_2 - f_2} + \left(\frac{f_2}{f_3}\right)^2 \Delta \tag{30}$$

where d_2 is the distance between M_2 and M_0. (Note that for perfect telescope adjustment, (30) yields the standard result for a flat output mirror, $2S_0 = f_2^2/(d_2 - f_2)$.) Therefore in order to have a stable resonator, Δ must satisfy the condition

$$\Delta > -2S_0 \left(\frac{f_3}{f_2}\right)^2. \tag{31}$$

It should be kept in mind that the beam waist at the gain medium is controlled by the stability range, and hence by Δ. In particular, too large Δ will lead to too large a beam waist.

The ratio of beam spot diameter at the grating to that at M_0 is given by the telescope magnification factor

$$m = m_o + \frac{\Delta}{f_3}\left[1 - \frac{d_g}{f_4}\right]. \tag{32}$$

Therefore when $\Delta = 0$, we obtain the classical magnification ratio.

III. Realization and Experimental Results

For our experiments we used $Tl^0(1)$ color centers [14] in KCl:Tl crystals (thickness ~1.7 mm) as the laser active medium [15], [16]. They present a broad absorption band peaking at 1.04 μm and can be efficiently pumped by the 1.06 μm Nd:YAG laser line. The laser emission has a broad tuning range (1.4 μm $< \lambda <$ 1.6 μm), peaking at 1.52 μm. For this spectral region (and in general for the infrared), high efficiency gratings are readily available. (With recently improved efficiencies of gratings in the visible spectrum [17], the method can be extended to CW dye lasers as well.)

The basic laser cavity is the astigmatically compensated, coaxially pumped cavity described in [18]. A single optical element (L_1M_1 in Fig. 1) was used as the pump beam focusing lens and input mirror. As mentioned earlier, $R_1 \sim 3.7$ mm; therefore $\Delta\nu_{hb} \cong 20$ GHz. Temporarily using a real mirror ($R = \infty$) for M_0($d_2 \sim 60$ cm), we maximized the output power. We then inserted an aperture in the long arm as a reference for further cavity modifications. The measured output beam radius was 0.6 mm, as expected from a beam waist radius in the crystal of ~20 μm. After this optimization L_1 M_1 and M_2 were kept untouched for all experiments.

We tested several possible telescope combinations where M_3 has radii of -120 and -200 mm, and M_4 had radii of 420, 500, and 1000 mm; the combinations (-120, 420 mm) and (-120, 500 mm) showed a better stability, and were easily alignable. Therefore, the maximum magnification used was ~4.2. Thus the beam diameter at the grating ($2w_g$) was limited to a value slightly less than 5 mm.

Two gratings were tested to increase even further the span of values of $\delta\nu$ given by (18), one with 830 g/mm [19] and another with 1200 g/mm [20]. For $\lambda = 1.5$ μm, these provided values for θ of ~38 and 64°, respectively. Both gratings were gold coated and presented an output coupling (0th order) of ~10 percent.

All the frequency spectra were analyzed using a scanning Fabry-Perot with a finesse greater than 100 and variable interplate distance.

Table I shows the measured mode frequency spacing $\Delta\nu$ and the measured beam spot diameter in the grating ($2w_g$) for various telescope-grating combinations. The calculated grating dispersion $\delta\nu$, given by (18), is also shown (see Table I). Note that as the grating dispersion increases ($\delta\nu$ decreases) the fundamental and competing modes come closer in frequency until single-mode operation is achieved ($\Delta\nu = 0$).

Estimating an internal loss of 10 percent, we can, using (22), obtain the gain at threshold ($g_t \sim 0.1$). Then with the measured value of $\Delta\nu$, we can obtain the maximum gain G (24). The results are shown in Table I. For the experiments with the 830 g/mm grating (lines 1 and 2 of Table I) we used CW pumping. The pump power was held to ~2 W since at higher powers, thermal effects tend to reduce the gain and to limit the output power. We see that in both cases, the maximum available gain was about the same. Fig. 5 shows the behavior of the gain, grating dispersion, and net gain as a function of the normalized frequency shift, $x(=\Delta\nu/\Delta\nu_{hb})$, for the pure CW case. We see that as we increase the grating selectivity ($R_1 \rightarrow R_2$) the net gain maximum is pulled closer to the main frequency (shown by the maxima of curves γ_1 and γ_2).

Perhaps it should be stated explicitly that for all the experiments described in Table I, the pump powers were always at least one order of magnitude above threshold.

In order to achieve higher gain and higher output powers, the pump beam (now ~5 W) was chopped with a 20 percent duty cycle. Introducing the more dispersive grating (line 3 of Table I) we obtained the time average frequency spectrum shown in Fig. 6, with two modes separated by 5.6 GHz. The extra, low-amplitude bump is attributed to mechanical instabilities, since the spectrum is time averaged. In single fast scans it was not observed.

Assuming the same net loss, we again, as described before, calculated the maximum available gain G (see Table I). Note that in the chopped pumping mode, G is 2.8 times greater than in pure CW pumping.

Finally, single-frequency operation was achieved by increasing the beam magnification (see line 4, Table I). The measured time average frequency spectrum is shown in Fig. 7.

Using the fact that the telescope does not introduce significant loss (we obtained approximately the same maximum gain with and without the telescope, as pointed out by lines 1 and

TABLE I

	Grating (g/mm)	Magnification $m_o = -\frac{R_4}{R_3}$	Beam Diameter $2w_g$ (mm)	$\Delta\nu$ (GHz)	$\delta\nu$	G
1[a]	830	1[c]	1.2	14.8	38.5	4.3
2[a]	830	4.2 = 500/120	4.2	10.8	28.6	4.2
3[b]	1200	3.5 = 420/120	4.2	5.6	12.8	11.6
4[b]	1200	4.2 = 500/120	4.8	0	9.6	
5[a]	1200	4.2 = 500/120	4.8	0	9.6	

[a] Pure CW pumping.
[b] Chopped pumping (duty cycle ~20 percent).
[c] No magnification is used. Grating positioned at M_0.

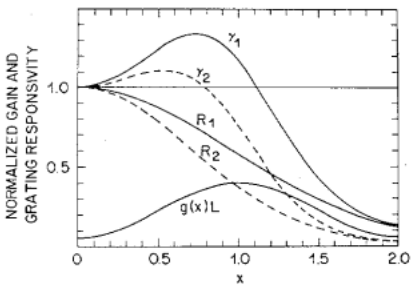

Fig. 5. The quantities gL and R (gain and grating response) and their resultant, γ, plotted as a function of the normalized detuning parameter, x for cases 1 and 2 of Table I (see text).

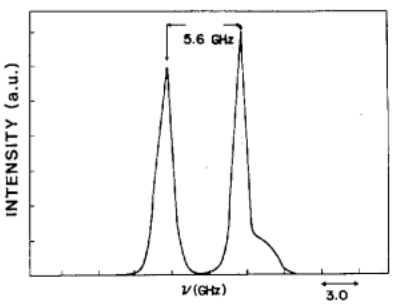

Fig. 6. Time average frequency spectrum of the laser output when using 1200 g/mm grating with w_g = 2.1 mm and chopped pumping (case 3 of Table I).

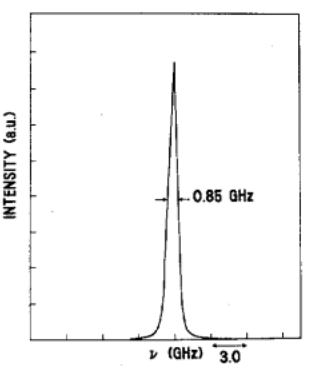

Fig. 7. Time average frequency spectrum of the laser output for case 4 of Table I.

2 of Table I), we can use the gain obtained under the conditions of line 3, Table I, to analyze the gain conditions in the vicinity of single-frequency operation. The results are plotted in Fig. 8. The net gain γ_3 is the result of the grating dispersion R_3 acting upon the gain gL, and at this point a maximum

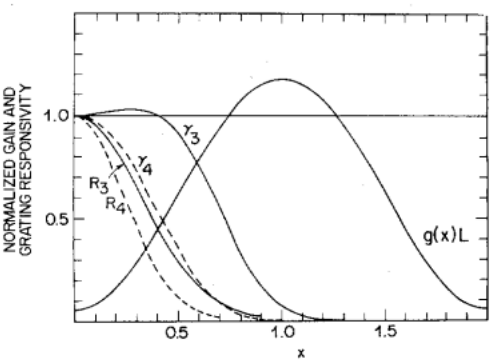

Fig. 8. Same as Fig. 5, for cases 3 and 4 of Table I, γ_4 represents the net gain for single-frequency operation.

above threshold is still observed. For an increased grating selectivity (line 4 of Table I), (shown as R_4), the resulting net gain γ_4 does not cross the threshold line any further, leading to single-frequency operation.

In fact, using the value of $\delta\nu$ for the single-frequency case, and the same net loss we see that [cf. (25)] the system would still operate in single frequency for maximum gain up to $G \leqslant 16.5$.

The experiment described in Table I, line 5 was performed in order to show the effects of reduced G on the true single-frequency operation. The resultant time average frequency spectrum is shown in Fig. 9. Note that the frequency width is much narrower (0.3 GHz) than in the chopped pumping case (0.85 GHz). This can be understood in terms of the increased sharpness of the net gain curve obtained in pure CW pumping, and the net resultant tighter control it has over cavity detuning due to mechanical and thermal instabilities. That is to say, the smaller the available gain, the sharper the net gain curve and the narrower the time average frequency spectrum. We also note, again, that the instantaneous frequency spectrum is much sharper than the time average behavior of Fig. 9.

As already indicated in the introduction, the *instantaneous* frequency spectrum is much sharper than the time average behavior shown in Fig. 9. That is, during lulls in vibration of the cavity mirrors, the observed line width was a small fraction of the cavity mode spacing (0.1 GHz). This observation constitutes further and very direct evidence that our laser had indeed achieved single-frequency operation. Once again, a greatly reduced time average bandwidth should be achievable, simply through use of a more mechanically stable cavity.

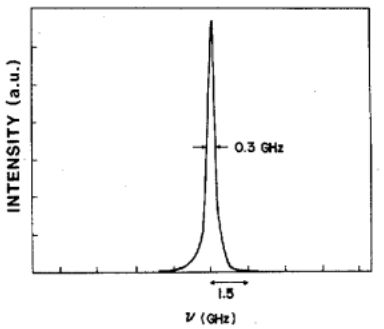

Fig. 9. Same as Fig. 6 for case 5 of Table I.

All the above results and analysis were carried out with the laser tuned to the peak of the laser emission band. As we scan the laser to the short wavelength side, the grating selectivity, $(\delta\nu^{-1})$, decreases. This effect is compensated by the decrease of the gain cross section, and the corresponding decrease in G. In fact, we did not observe deviations from single-frequency operation when scanning through the gain curve.

Finally, we must point out that increasing the output coupling reduced the required G to achieve single-frequency operation [see (26)]; in addition it increases the amount of traveling waves inside the resonator. These homogeneously depopulate the gain medium, thereby reducing the population for the competing mode. Again, the requirements for single-frequency operation are overestimated in our calculations.

References

[1] R. V. Schmidt, D. C. Flanders, C. V. Shank, and R. D. Stanley, "Narrow-band grating filters for thin-film optical wave-guides," *Appl. Phys. Lett.*, vol. 25, pp. 651–652, Dec. 1974.

[2] C. L. Tang, H. Statz, and G. Demars, "Spectral output and spiking behavior of solid-state lasers," *J. Appl. Phys.*, vol. 34, pp. 2289–2295, Aug. 1963.

[3] H. Statz and C. L. Tang, "Multimode oscillations in solid state masers," *J. Appl. Phys.*, vol. 35, pp. 1377–1383, May 1964.

[4] C. T. Pike, "Spatial hole burning in cw dye lasers," *Opt. Commun.*, vol. 10, pp. 14–17, Jan. 1974.

[5] H. W. Schroder, H. Dux, and H. Welling, "Single mode operation of cw dye lasers," *Appl. Phys.*, vol. 7, pp. 21–28, Feb. 1975.

[6] I. V. Hertel, W. Muller, and W. Stoll, "A kinematic model for the oligomode action of a CW dye laser," *IEEE J. Quantum Electron.*, vol. QE-13, pp. 6–9, Jan. 1977.

[7] F. P. Schafer, Ed., *Dye Lasers.* New York: Springer-Verlag, 1973, pp. 66–79.

[8] W. Demtroder, Ed., *Laser Spectroscopy.* New York: Springer-Verlag, 1981, sec. 7.3.5, pp. 349–353.

[9] K. W. Giberson, C. Cheng, F. B. Dunning, and F. B. Tittle, "Tunable single-mode operation of a cw color center laser in the near infrared," *Appl. Opt.*, vol. 21, pp. 172–173, Jan. 1982.

[10] K. R. German, "Grazing angle tuner for cw lasers," *Appl. Opt.*, vol. 20, pp. 3168–3171, Sept. 1981.

[11] K. R. German, "Polarization beam splitters for pumping of FII-center lasers," *Opt. Lett.*, vol. 4, pp. 68–69, Feb. 1979.

[12] H. W. Kogelnik, E. P. Ippen, A. Dienes, and C. V. Shank, "Astigmatically compensated cavities for CW dye lasers," *IEEE J. Quantum Electron*, vol. QE-8, pp. 373–379, Mar. 1972.

[13] H. W. Kogelnik, "Imaging of optical modes–Resonators with internal lenses," *Bell Syst. Tech. J.*, vol. 44, pp. 455–494, Mar. 1965.

[14] L. F. Mollenauer, N. D. Vieira, Jr., and L. Szeto, "Optical properties of the $Tl^0(1)$ center in KCl," *Phys. Rev. B*, vol. 27, pp. 5332–5346, May 1983.

[15] W. Gellerman, F. Luty, and C. R. Pollack, "Optical properties and stable broadly tunable cw laser operation of new F_A-type centers in Tl^+ doped alkali halides," *Opt. Commun.*, vol. 39, pp. 391–395, Nov. 1981.

[16] L. F. Mollenauer, N. D. Vieira, and L. Szeto, "Mode locking by synchronous pumping using a gain medium with microsecond decay times," *Opt. Lett.*, vol. 7, pp. 414–416, Sept. 1982.

[17] D. Maystre, J. P. Laude, P. Gacoin, D. Lepere, and J. Priou, "Gratings for tunable lasers using multidielectric coatings to improve their efficiency," *Appl. Opt.*, vol. 19, pp. 3099–3102, Sept. 1980.

[18] L. F. Mollenauer and D. H. Olson, "Broadly tunable lasers using color centers," *J. Appl. Phys.*, vol. 46, pp. 3109–3118, July 1975.

[19] The grating and sine-drive mounting are available from Burleigh Instruments, Inc., Fishers, NY.

[20] Gold coated, copper substrate Bausch & Lomb grating catalog number 35-53-*-340.

[21] See, for example, K. Lin and M. G. Littman, "A novel geometry for single mode scanning of tunable lasers," *Opt. Lett.*, vol. 6, pp. 117–118, Mar. 1981.

Nilson Dias Vieira, Jr. was born in 1953 in São Paulo, Brazil. He received the M.Sc. degree in physics from the University of São Paulo in 1979.

Since 1979 he has been a member of staff of the Instituto de Psequisas Energéticas e Nucleares, São Paulo. He has recently returned to São Paulo following a two year visit at Bell Laboratories, Holmdel, NJ. He soon expects to receive the Ph.D. degree in physics.

Linn F. Mollenauer M'78) received the B.Eng. physics degree from Cornell University, Ithaca, NY, in 1959 and the Ph.D. degree in physics from Stanford University, Stanford, CA, in 1965.

Since joining the technical staff of Bell Laboratories, Holmdel, NJ, in 1972, his work has focused on the color center laser and on the study of nonlinear effects in optical fiber pulse propagation; a recent outgrowth of that work is his invention of the soliton laser.

Dr. Mollenauer is a member of the American Physical Society, and is a Fellow of the American Association for the Advancement of Science and of the Optical Society of America. He was awarded the 1982 R. W. Wood Prize of the Optical Society of America for his pioneering work on the color center laser, and he has also received the Bell Laboratories Distinguished Technical Staff Award.